NJC

ROYAL SOCIETY OF CHEMISTRY

PAPER

View Article Online
View Journal | View Issue

Cite this: *New J. Chem.*, 2023, **47**, 7622

Novel histone deacetylase 6 inhibitors using benzimidazole as caps for cancer treatment†

Phuong Hong Nguyen,‡[ab] Bui Thi Buu Hue,‡*[c] Minh Quan Pham,‡[de] Tran Phuong Hoa,[ab] Quang De Tran,[c] Hosun Jung,[ab] Le Trong Hieu,[c] Nguyen Cuong Quoc,[c] Hong Vinh Quang,[c] Nguyen Phu Quy,[c] Hye Jin Yoo[a] and Su-Geun Yang*[ab]

Received 22nd November 2022,
Accepted 23rd February 2023

DOI: 10.1039/d2nj05731j

rsc.li/njc

Histone deacetylases (HDACs) have proven to be promising targets for the development of anticancer drugs. In this work, we report the design and synthesis of a series of 19 novel hydroxamic acid-based histone deacetylase inhibitors conjugated to benzimidazole and benzoxazole core structures. Five compounds showed anti-proliferative activity with an IC_{50} value of 2.9–70.9 μM. Compound **7** displayed the highest efficacy against MCF-7 cells and exhibited antiproliferative effects against a panel of cancer cell lines. Compound **7** was the most potent selective inhibitor of HDAC6 and had an IC_{50} value 8- to >111.1-fold those of HDAC3, HDAC4, HDAC8, and HDAC11, and was a superior HDAC6 inhibitor to belinostat. Its interaction with and inhibitory activity on HDAC enzymes were then explored in a molecular docking study. The obtained data revealed the highest binding affinity (−8.46 kcal mol^{-1}) of compound **7** toward HDAC6, as it formed interactions with the key residues Cys584 and Asp612 within the active site. Furthermore, the HDAC inhibitory activity of compound **7** was demonstrated from the dose-dependent increase in the tubulin acetylation level. Together, our results indicated that compound **7** with a cap of benzimidazole and four carbon-chain-containing thioether linker is a potent anticancer agent for selective HDAC6 inhibition and deserves further investigation.

Introduction

Histone deacetylases (HDACs) are a family of enzymes that play important roles in different biological processes, mainly because of their transcription-repressive activities. Dysregulation in HDAC activity to regulate various cellular processes, including survival, differentiation, and apoptosis, has been reported in several forms of cancers.[1] Furthermore, HDACs regulate the expression and activity of numerous proteins involved in cancer initiation and progression. Therefore, HDACs are considered as promising therapeutic agents for developing antitumor therapy because of their key roles in the onset and progression of cancers.[2] The HDAC family comprises 18 members categorized into four groups, namely, class I (HDACs 1, 2, 3, and 8), class II (class IIa [HDACs 4, 5, 7, and 9], class IIb [HDACs 6 and 10], and class IV [HDAC11]).[3] At present, several HDAC inhibitors (HDACIs) have been reported, most of which have a common structural model with three parts: a surface recognition cap group which interacts with amino acids near the entrance of the active site, a saturated or unsaturated linker that occupies the narrow hydrophobic channel and a zinc binding group (ZBG) that chelates the active site Zn^{2+} ions (Fig. 1A).[4] Among the potent HDACIs, hydroxamic acid containing organic molecules display a strong affinity toward histone deacetylase due to their strong metal ion chelating properties. Various molecules bearing free hydroxamic acid at one terminal have been synthesized and evaluated for their activities, and some of them are licensed or are at various stages of clinical evaluation.[5] However, most of these molecules are class I selective (FK-228, PXD-101) or pan-HDAC inhibitors (SAHA, LBH-589).[6] Targeting multiple HDAC isoforms simultaneously might cause undesirable side-effects, as is observed for approved broad-spectrum HDACIs; therefore, isoform-selective compounds have particularly gained increased attention as a preferred target.[7]

[a] *Department of Biomedical Science, BK21 FOUR Program in Biomedical Science and Engineering, Inha University College of Medicine, Incheon 22212, Korea. E-mail: sugeun.yang@inha.ac.kr*
[b] *Inha Institute of Aerospace Medicine, Inha University College of Medicine, Incheon 22332, Korea*
[c] *College of Natural Sciences, Can Tho University, Can Tho city, Vietnam. E-mail: btbhue@ctu.edu.vn*
[d] *Institute of Natural Products Chemistry, Vietnam Academy of Science and Technology, Ha Noi, Vietnam*
[e] *Graduate University of Science and Technology, Vietnam Academy of Science and Technology, Ha Noi, Vietnam*

† Electronic supplementary information (ESI) available. See DOI: https://doi.org/10.1039/d2nj05731j

‡ Equal contribution.

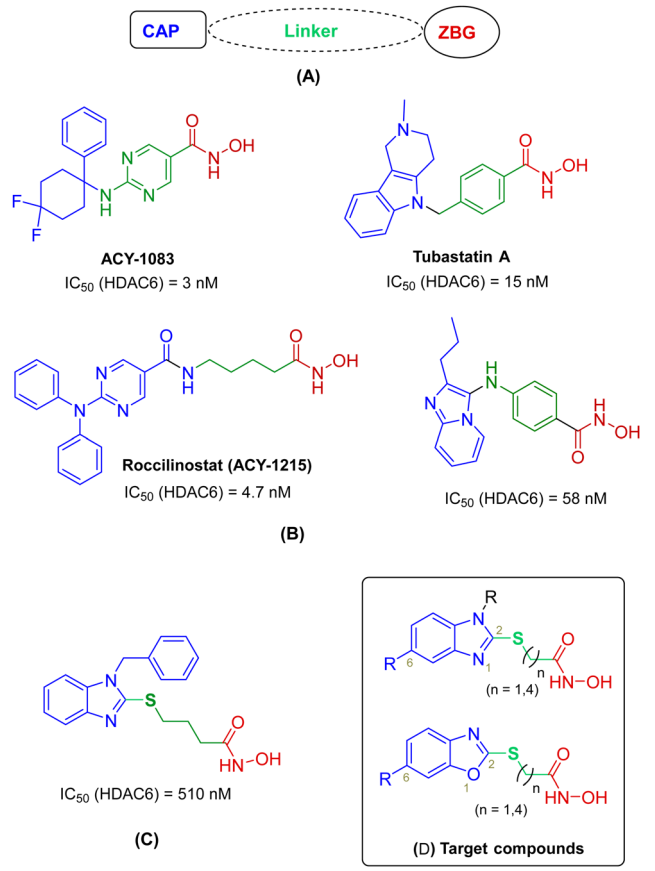

Fig. 1 (A) Basic pharmacophore features of HDACIs; (B) and (C) selective HDAC6 inhibitors; (D) design for hydroxamate conjugated benzimidazole and benzoxazole and general structures of the target compounds.

HDAC6 has a unique activity profile compared to other HDACs and is usually localized in the cytoplasm. It contains two catalytic sites and a ubiquitin-binding domain that removes the acetyl group from lysine residues in non-histone substrates, including α-tubulin and Hsp90.[8,9] Contrary to the lethal effects of HDAC1–3 genetic ablation, HDAC6 showed a normal phenotype and was viable in knock out mice.[10] Indeed, HDAC6 inhibitors seems to be less cytotoxic toward mammalian cells and may have fewer side-effects than pan-HDAC inhibitors and HDAC1–3 selective inhibitors.[11] To date, several HDAC6-selective inhibitors have been reported.[5f,11b,12] HDAC6 is a potential new target for a growing number of diseases with different pathophysiologies. The inhibition of HDAC6 could be a viable approach to reduce the toxicity associated with pan-HDAC inhibitors. Therefore, the design of HDAC6 inhibitors seems to be more appropriate than that of other isoforms, and several selective HDAC6 inhibitors have been developed (Fig. 1B).[13] These HDAC6 inhibitors were designed and synthesized by modifying the nature of the cap structural entity and attaching a short benzyl or 4-aminophenyl linker. *N*-heterocyclic ring systems including benzimidazoles[14] and benzoxazoles[15] are known as cap portions of novel HDACIs with potent anticancer activities. Shaymaa *et al.* previously described a benzimidazole-based HDAC6 inhibitor carrying 2-mercaptobenzimidazole key building blocks that exhibited an IC_{50} value of 510 nM (Fig. 1C).[16] However, the synthesis procedure is limited to unsubstituted C-5 benzimidazoles, while most biologically active benzimidazole-based compounds bear functional groups at the 1, 2, and/or 5/6 positions.[17] In addition, the alkylation reactions of NH and SH gave low yields, likely owing to the competition between these two positions toward alkylating reagents.

Herein, we report the development of a synthetic pathway that allows for rapid and diversity-oriented synthesis of target benzimidazole- and benzoxazole-based hydroxamates that lead to potent and selective HDAC6 inhibitors with antiproliferative activity against nine diverse cancer cell lines. Docking studies allowed rationalization of the observed selectivity profile.

1. Experimental section

1.1. Chemistry

1.1.1. General information. Reactions were monitored by thin-layer chromatography (TLC) on 0.2 mm pre-coated silica-gel 60 F254 plates (Merck). ^{1}H nuclear magnetic resonance (NMR) and ^{13}C NMR spectra were measured on Bruker Avance 300 MHz, Bruker Avance 500 MHz, and Bruker Avance 600 MHz spectrometers. Mass spectrometry (MS) data were recorded on an 1100 series LC-MSD-Trap-LS Agilent spectrometer, and high-resolution electrospray ionization mass spectrometry (HRESI-MS) observations were performed on a Bruker MicrOTOF-Q mass spectrometer. Fourier transform infrared (FT-IR) spectroscopy was conducted as per the KBr pellet method on a Thermo Nicolet 6700 spectrometer. Chemical shifts are shown in parts per million (ppm) relative to tetramethylsilane (Me4Si, $\delta = 0$); J values are given in Hertz.

Appendix A. Supplementary data.

1.2. Biological methods

1.2.1. Antiproliferative assay. The MCF-7 cell line was obtained from ATCC. The cells were cultured *in vitro* in DMEM (Invitrogen, Paisley, UK) containing 10% fetal bovine serum (Gibco) and 1% penicillin. For cytotoxicity assays, MCF-7 cells were seeded into 96-well culture plates at 3×10^5 cells per well in 0.1 mL of DMEM and incubated at 37 °C with 5% CO_2 and 90% humidity. After 16 h, the cells were treated with drugs (250 μM concentration, serially diluted up to three-fold) for 48 h. Cell viability was measured using the CELLOMAXTM Viability Assay kit (Precaregene, Korea). UV absorption at 450 nm wavelength was measured using an Infinite M200 microplate reader (Tecan, Zürich, Switzerland). The IC_{50} values were calculated using Prism v7.0. The inhibitory activity of the tested compounds was evaluated *via* an 8-point dose response curve (DRC) analysis in triplicate.

The antiproliferative activities of compounds **7** and **27** against seven solid tumor cell lines, human ovarian cancer SKOV-3 cells, breast cancer MCF-7, MDA-MB-231, EMT6 cell lines, liver cancer Hepa1c1c7 cells, lung cancer A549 cells, pancreatic cancer PANC1 cells, and brain N2a cells were evaluated using the CELLOMAXTM Viability Assay kit, and belinostat was used as the positive control.

1.2.2. HDAC enzyme inhibition assays. The compounds, diluted to the indicated concentrations, were mixed with HDAC enzymes (HDAC1, HDAC3, HDAC6, HDAC8, and HDAC11) and the substrate for 1 h (PBS Biosciences). The fluorescence intensity was measured according to the manufacturer's instructions. The inhibition rates of the test compounds were calculated based on the dimethyl sulfoxide (vehicle)-treated group and positive control (belinostat) group.

1.2.3. Western blotting. MCF-7 and N2a cell lines were incubated with various concentrations of test agents for 6 h. Cell lysis and western blot analyses were performed as previously described. Anti-acetylated tubulin antibody and horseradish peroxidase (HRP)-conjugated secondary antibodies (Santa Cruz Biotechnology) were used. Immunoreactive bands were visualized using enhanced chemiluminescence (Millipore, USA).

1.3. Molecular docking studies

1.3.1. Ligand and receptor preparation. The three-dimensional structures of the ligands were prepared using MarvinSketch version 19.27.0 and PyMOL version 1.3r1.[18] Energy minimization was carried out using the MM2 force field, and quantum chemical calculations were performed at the B3LYP/6-31g(d,p) level implemented in Gaussian 09.[19] Belinostat was previously reported as a novel inhibitor of histone deacetylase; thus, it was selected as the reference ligand for docking simulation.[20]

The PDB entries chosen for docking studies 4A69 (HDAC3),[21] 4CBT (HDAC4),[22] 5EEI (HDAC6),[23] and 1T67 (HDAC8)[24] were obtained from the PDB archive. The amino acid sequence of HDAC11 was already well determined, and its information is publicly available at the National Center for Biotechnology Information (NCBI) archived under entry ID: NP_079103.2. The crystal structure of human HDAC11 was built and validated using the Swiss-Model webserver (https://swissmodel.expasy.org). The Graphical User Interface program Autodock Tools 1.5.6 (ADT) was employed to set up the input data. Details of the molecular docking simulation are provided in the ESI.†

1.3.2. Docking using AutoDock4Zn. In the grid parameters, an autogrid was carried out to pre-calculate grid maps of the interaction energies between the atoms of the ligand and protein. The receptor grid preparation for the docking procedure was implemented by assigning the zinc ion as the center of the grid box and comprised 64 × 64 × 64 points with 0.375 Å

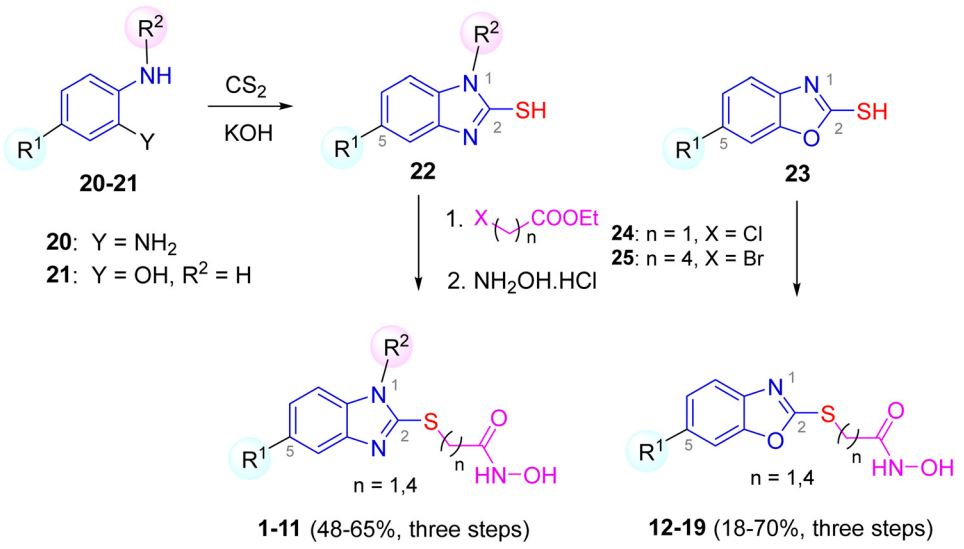

Compd.	R^1	R^2	n	Total yield (%)
1	H	H	4	50
2	Cl	H	4	61
3	OCH_3	H	4	48
4	H	Bn	4	60
5	CF_3	Bn	4	66
6	CF_3	*o*-Cl-Bn	4	58
7	H	*o*-Cl-Bn	4	57
8	H	Bn	1	58
9	CF_3	Bn	1	65
10	CF_3	*o*-Cl-Bn	1	59
11	H	*o*-Cl-Bn	1	57

Compd.	R^1	n	Total yield (%)
12	H	1	43
13	CH_3	1	69
14	Cl	1	18
15	F	1	42
16	OCH_3	1	50
17	H	4	56
18	CH_3	4	70
19	OCH_3	4	57

Scheme 1 Synthesis of benzimidazole/benzoxazole based hydroxamates.

spacing. The grid input file also included AD4Zn.dat, which is a specific parameter file for zinc ions. The molecular docking study utilized AutoDock4Zn[25] with the Lamarckian genetic algorithm (LGA) to search for the optimum docking pose together with a scoring function to calculate the binding affinity. A total of 50 runs were performed for each docking, and the remaining parameters were set to default values.

2. Results and discussion

2.1. Structural design and synthesis

To investigate the structure–activity relationship (SAR) of the cap and the linker region, we designed two series of HDACIs that used benzimidazole and benzoxazole analogs as the capping group and two different types of linkers. The general structures of the target compounds are shown in Fig. 1D. In these two structures, the hydroxamate ZBG moiety was incorporated at C-2 of the heterocycle through saturated one- or four-carbon containing thioether linkage. Different substituted benzyl moieties were introduced at the position N-3 of the benzimidazole ring, and electron-donating groups (CH_3, OCH_3) or electron-withdrawing groups (Cl, F, CF_3) were added to the position C-5 of the heterocycle rings to investigate their electronic effects on activities. These designs are expected to increase binding to HDAC enzymes and consequently enhance potency and selectivity as well as to decrease toxicity and improve bioavailability.

The target benzimidazole- (**1–11**) and benzoxazole-based hydroxamic acids (**12–19**) were synthesized *via* a three-step pathway, as depicted in Scheme 1.

In the first step, *N*-benzyl *o*-phenylenediamines **20**[17b,26] or commercially available *o*-aminophenol **21** was condensed with CS_2 under basic conditions (KOH in ethanol) to obtain the corresponding benzimidazolethiols **22** and **23**, respectively.[16] The thiol moieties were then coupled with ethyl 2-chloroacetate **24** or ethyl 5-bromopentanoate **25** *via* nucleophilic substitution under basic conditions (K_2CO_3). This process resulted in the incorporation of ester functions that were eventually subjected to aminolysis with hydroxyamine[27] to afford the desired thioether linked hydroxamate conjugated benzimidazoles **1–11** or benzoxazoles **12–19**, respectively, in moderate to good total yields over three steps. The synthetic results of the benzimidazole derivatives (compounds **1–11**) indicated that electron-withdrawing (Cl, CF_3) or electron-donating (OCH_3) groups on the benzene ring or/and the benzyl group on the nitrogen of *o*-phenilenediamines **20** assisted the ring closure process while the length of the alkyl side chain seemed likely not to affect the yield of this step (Scheme S1, ESI†). However, the methoxy group (OCH_3) appeared not to tolerate the reaction conditions of the aminolysis step, which resulted in lowering of the total yield of the final product (compound **3**). Almost the same results were also observed in the case of benzoxazole derivatives (**12–19**) except that the lower yield of the final aminolysis step had probably something to do with the presence of the halogen groups (Cl, F) (Scheme S2, ESI†).

Table 1 Inhibition screening results

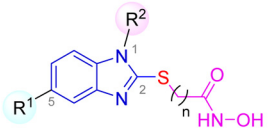

1-11

12-19

Compd	R^1	R^2	n	IC_{50}[a] (μM)	I_{max} (%)
1	H	H	4	ND	3.0
2	Cl	H	4	ND	20.0
3	OCH_3	H	4	ND	3.0
4	H	Bn	4	ND	23.0
5	CF_3	Bn	4	28.43 ± 1.18	96.9
6	CF_3	*o*-Cl-Bn	4	15.63 ± 1.09	98.1
7	H	*o*-Cl-Bn	4	2.91 ± 1.40	94.8
8	H	Bn	1	ND	25.0
9	CF_3	Bn	1	ND	4.0
10	CF_3	*o*-Cl-Bn	1	50.46 ± 1.14	67.15
11	H	*o*-Cl-Bn	1	70.96 ± 1.16	85.5
12	H	—	1	ND	40.0
13	CH_3	—	1	ND	31.0
14	Cl	—	1	ND	44.0
15	F	—	1	191 ± 1.60	46.0
16	OCH_3	—	1	ND	38.0
17	H	—	4	ND	20.0
18	CH_3	—	4	ND	40.0
19	OCH_3	—	4	ND	32.0
Belinostat	—	—	—	2.6 ± 1.40	100

[a] IC_{50} values were calculated by 8-point DRC analysis in duplicate. Experiments were repeated at least two time independently. I_{max} (%) indicates inhibitory maximum.ND: Not determined.

2.2. Inhibition screening

The MCF-7 cell line was obtained from the American Type Culture Collection (ATCC) and cultured *in vitro* in Dulbecco's modified Eagle's medium (DMEM; Invitrogen, Paisley, UK) containing 10% fetal bovine serum (Gibco) and 1% penicillin. Cells were treated with different compounds **(1–19)** at a concentration of 250 μM with three-fold serial dilutions and further incubated for 48 h. The screening results are shown in Table 1. Compounds **5** and **6** showed moderate cytotoxicities with IC_{50} values of 28.43 and 15.63 μM, respectively. Remarkably, compound **7** exhibited the best activity with an IC_{50} value of 2.91 μM, which was comparable to that of the positive control belinostat (IC_{50} = 2.6 μM).

2.3. Antiproliferative activity

The antiproliferative activity of compound **7** against a variety of cells of solid tumors was then evaluated, and belinostat was the positive control. Compound **7** showed antiproliferative effects against all tested cell lines with the IC_{50} values ranging from 2 to 17 μM (Table 2). Previously, a selective HDAC6 inhibitor ACY-1215 also showed weaker anti-proliferative activities against a variety of cells compared to the pan-HDAC inhibitor.[6] In the next data, we will investigate their specificity against HDAC isoforms.

2.4. *In vitro* HDAC isoform inhibition activity

Compound **7** was evaluated for its inhibitory activity against HDAC3, HDAC4, HDAC6, HDAC8, and HDAC11 isoforms; belinostat served as the positive control (Fig. 2 and Table 3).

Table 2 Antiproliferation of compounds on different cell lines

Tumor cell	Cell line	IC_{50}[a] (μM) Compound 7	Belinostat
Breast	MDA-MB-231	2.95 ± 0.01	0.52 ± 0.01
Breast	EMT6	6.77 ± 0.1	1.29 ± 0.5
Brain	N2A	4.21 ± 0.1	3.13 ± 0.1
Liver	Hepa1c1c7	9.05 ± 0.25	1.31 ± 0.2
Ovarian	SKOV3	12.5 ± 0.7	4.47 ± 0.1
Colon	SW620	14.8 ± 1.8	0.8 ± 0.01
Pancreas	PANC1	17.2 ± 1.01	12.8 ± 0.75

[a] IC_{50} values were calculated by 8-point DRC analysis in duplicate. Experiments were repeated at least two time independently.

Compound 7 showed inhibitory activity against all HDACs. Compound 7, with a cap of benzimidazole and a four-carbon-containing thioether linker, served as the most potent agent with an IC_{50} value of 0.09 μM for HDAC6. In contrast, the pan-selective inhibitor belinostat was weaker than compound 7, with an IC_{50} value of 0.17 μM. Compound 7 exhibited the most potent selectivity for HDAC6 as compared to class I HDAC3 (20-fold) and HDAC8 (8.1-fold), class IIa HDAC4 (>111.1-fold), and class IV HDAC11 (>111.1-fold). The HDAC6 selectivity of 7 is superior to belinostat. These data suggest that the enzymatic activity and cellular activity are qualitatively less correlated. Compound 7 shows a similar trend to ACY-1215, a first-in-class isoform-selective HDAC6 inhibitor that showed weaker anti-proliferation against various tumor cell lines compared to belinostat.[6] These results indicate that compound 7 is a potential selective HDAC6 inhibitor.

2.5. Selective upregulation in the acetylation level of tubulin

The effect of compound 7 and belinostat as a positive control on the acetylation of α-tubulin (a known substrate for HDAC6), a biomarker of HDAC inhibition, in MCF-7 and N2a cells was measured by western blotting (Fig. 3). As shown in Fig. 3, compound 7 induced Ac-α-tubulin increased Ac-α-tubulin levels in a dose-dependent manner. These data confirmed the selectivity profile of compound 7 at the cellular translational level.

2.6. The SAR analysis

By comparing the cytotoxicity of the compounds reported in Table 1, the following structure activity relationships (SAR) were suggested. Benzimidazole-based hydroxamate derivatives with one carbon alkyl chain as the linker (compds **8–11**) together with all benzoxazole derivatives were generally inactive. Similar results were also observed for compounds with four carbon-length chain linked to *N*–H or *N*-benzyl benzimidazoles (compds **1–4**). However, the introduction of an electron-withdrawing group such as CF_3 at the C-5 position (compound **5**) could actually induce measurable activity (IC_{50} = 28.43 μM) as compared to that of compound **1**. Remarkably, the presence of the Cl group on the benzene ring at the N-3 position (compound 7) led to a nearly 10-fold decrease in the IC_{50} value (IC_{50} = 2.91 μM) as compared to that of compound **5**, which was consistent with the positive control belinostat (IC_{50} = 2.6 μM). Surprisingly, the presence of the two substituents Cl and CF_3 in the molecule (compound **6**) led to five-fold decrease in activity compared to compound 7.

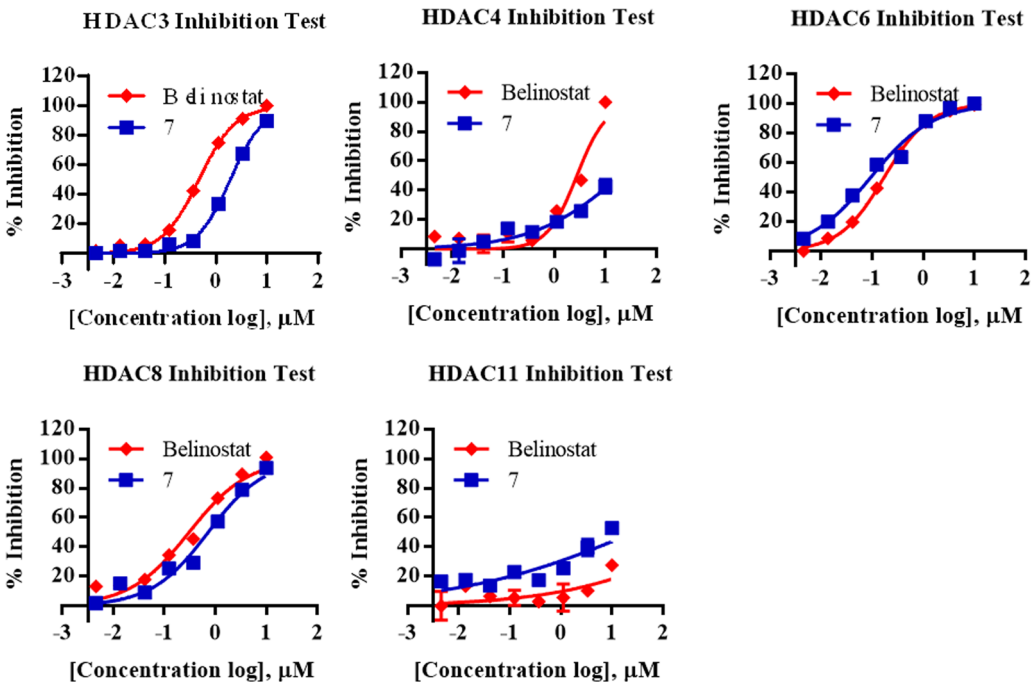

Fig. 2 HDAC inhibition activity of compound. Representatives DRCs (dose response curves) of 7 (blue color) and reference belinostat (red color). Percentage inhibition is shown in each graph. Compounds were tested in the 8-dose IC_{50} mode in duplicate with 3-fold dilutions starting at 10 μM. The inhibition was calculated as mentioned in the Materials and methods.

Table 3 HDACs inhibition activity of compound **7**. The IC_{50} values were calculated by DRC- analysis in duplicate. Experiments were repeated at last two times independently

	IC_{50} (μM)					Selective fold			
	HDAC3 (Class I)	HDAC8 (Class I)	HDAC4 (Class IIa)	HDAC6 (Class IIb)	HDAC11 (Class IV)	HDAC3/HDAC6	HDAC4/HDAC6	HDAC8/HDAC6	HDAC11/HDAC6
7	1.80 ± 0.06	0.73 ± 0.02	>10	0.09 ± 0.01	>10	20.00	>111.1	8.11	>111.1
Belinostat	0.45 ± 0.01	0.34 ± 0.06	2.70 ± 0.12	0.17 ± 0.02	>10	2.65	15.88	2.00	>58.82

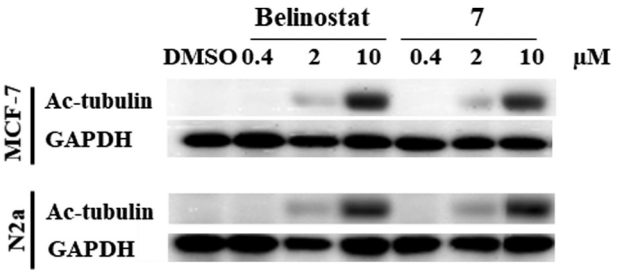

Fig. 3 Western blot analysis of acetylated α-tubulin (HDAC6 substrate) in MCF-7 and N2a after 6 h of treatment with compound **7** and belinostat at 10, 2, and 0.4 μM. GAPDH was used as a loading control.

In summary, hydroxamate **7** bearing benzimidazole as the cap pharmacophore exhibited good cytotoxicity against MCF-7 cells and had potency comparable to that of belinostat. This compound has crucial structural features, including a halogen (Cl) group on the benzene ring at the N-3 position of the heterocycle and a four-carbon containing thioether as a linker.

2.7. Docking study

Amongst the various docking software programs, AutoDock4 is a non-commercial package that has been widely used with more than 6000 citations during the last 10 years. This is a useful tool to rapidly predict the binding affinity of ligands toward a specific protein/enzyme target.[28] Given the increase in the demand among scientists to study metalloproteins, a new version, AutoDock4Zn, has been developed with improvements in the AutoDock force field for small-molecule docking to zinc metalloproteins.[25] As HDACs are well-known metalloproteins with zinc ions included within the active site, AutoDock4Zn was utilized to study the binding mechanism of the test compounds with these enzymes.

According to the ranking criteria of Autodock4, the more negative the docking energy, the better is the binding affinity of the compound toward the targeted receptor.[28a,29] The detailed docking pose analysis is presented in Table 4.

Regarding HDAC class I, including HDAC3 and HDAC8, the studied ligands showed common hydrogen bonds with essential residues within the active site of HDAC3 (Gly143, His172) and HDAC8 (Cys153, Asp178). Previous studies have indicated that His142, Cys153, Asp178, His180, and Phe208 are key residues of HDAC8 and participate in the formation of interactions with this ligand.[24,30] In particular, compound **7** exhibited a weaker binding affinity toward these targets than belinostat (−7.31; −9.78 kcal mol^{-1} for HDAC3 and −7.57; −8.13 kcal mol^{-1} for HDAC8, respectively), indicating that it may inhibit the function of targeted enzymes at a concentration higher than that of the reference ligand (Fig. 4). Binding orientation analysis of the studied ligands with HDAC4 (Class IIa) showed that belinostat docked to this enzyme at a higher binding affinity than compound **7**. In addition, the obtained data confirmed that compound **7** did not form H-bonds with the key residues at the active site, indicating that it is not a potential inhibitor of HDAC4 (Table 3).

Binding mode analysis of compounds with HDAC6 (Class IIb) revealed the best dock score for compound **7** (−8.46 kcal mol^{-1}), followed by belinostat (−8.00 kcal mol^{-1}). It should be noted that compound **7** and belinostat formed the same H-bonding toward Asp612 within the binding site of HDAC6. However, compound **7** formed one hydrogen bond with Cys584 different from that formed by belinostat, suggesting that this interaction might enhance the inhibitory activity. The results of the biological experiment correlated with the docking results where the IC_{50} of compound **7** was calculated to be 0.09 μM. Thus, these amino acids might play a significant role in the function of the targeted enzyme (Fig. 5).

Table 4 Docking results of studied compounds and hydrogen bond interacting residues

	Dock score (kcal mol^{-1})		H-bond interacting residues	
Enzyme	Compound **7**	Belinostat	Compound **7**	Belinostat
Class I				
HDAC3	−7.31	−9.78	Gly143, His172, Tyr298	Gly143, Cys145, His172
HDAC8	−7.57	−8.13	His142, Cys153, Asp178, His180	Gly140, Cys153, Asp178, Gln263
Class IIa				
HDAC4	−6.62	−8.62	His803	His802, His803, Phe871, Asp934, Pro942
Class IIb				
HDAC6	−8.46	−8.00	Cys584, Asp612	His573, His574, Asp612, His614
Class IV				
HDAC11	−7.02	−6.56	Gly619	Cys621, Asp649

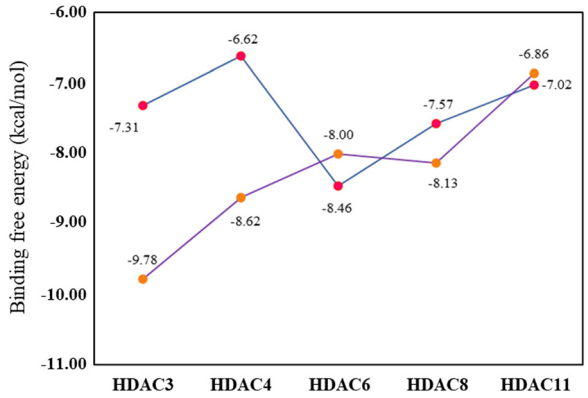

Fig. 4 Plot of ligand's binding free energy between compound **7** (blue line and pink dot) and belinostat (purple lines and orange dots) toward studied HDAC enzymes.

As the X-ray structure of HDAC11 was not characterized, we built a three-dimensional structure of HDAC11 by homology modeling on the Swiss-Model webserver (ESI† S2). It is commonly assumed that a good quality model is expected to have a score of over 90% in the most favored regions.[31] The data obtained from the Ramachandran plot showed that 91.69% amino acid residues of the HDAC11 model were located in the most favored regions (Fig. S2.1, ESI†); thus, it could be considered as a suitable model for further docking studies. Docking score analysis of the studied compounds with HDAC11 (Class IV) revealed that Gly619, Cys621, and Asp649 formed three H-bonds; however, the low binding affinity of both ligands suggests that they might not have the potential to inhibit the function of this enzyme (−7.02 and −6.86 kcal mol^{-1}, respectively).

3. Conclusions

To develop novel HDAC6 selective inhibitors with a benzimidazole cap group, nineteen hydroxamic acid conjugated benzimidazole or benzoxazole derivatives were prepared and evaluated for their bioactivities. Compound 7, with a cap of benzimidazole and a four-carbon containing thioether linker, showed the highest anticancer effect on cells. Antiproliferation assay revealed the potency of compound 7 against diverse cancer cell lines. The inhibitory activity of the title compound on HDAC isoforms (3, 4, 6, 8, and 11) and SAR analysis confirmed that the strategy successfully achieved the goal of finding a novel selective and highly efficient small molecule inhibitor of HDAC6. Compound 7 displayed the highest potency (at least eight-fold selectivity) for HDAC6 over other isoforms and is superior to belinostat. At the translational level, our western blot analysis further confirmed the increase in the acetylation level of α-tubulin, a substrate of HDAC6. Molecular docking studies indicated that

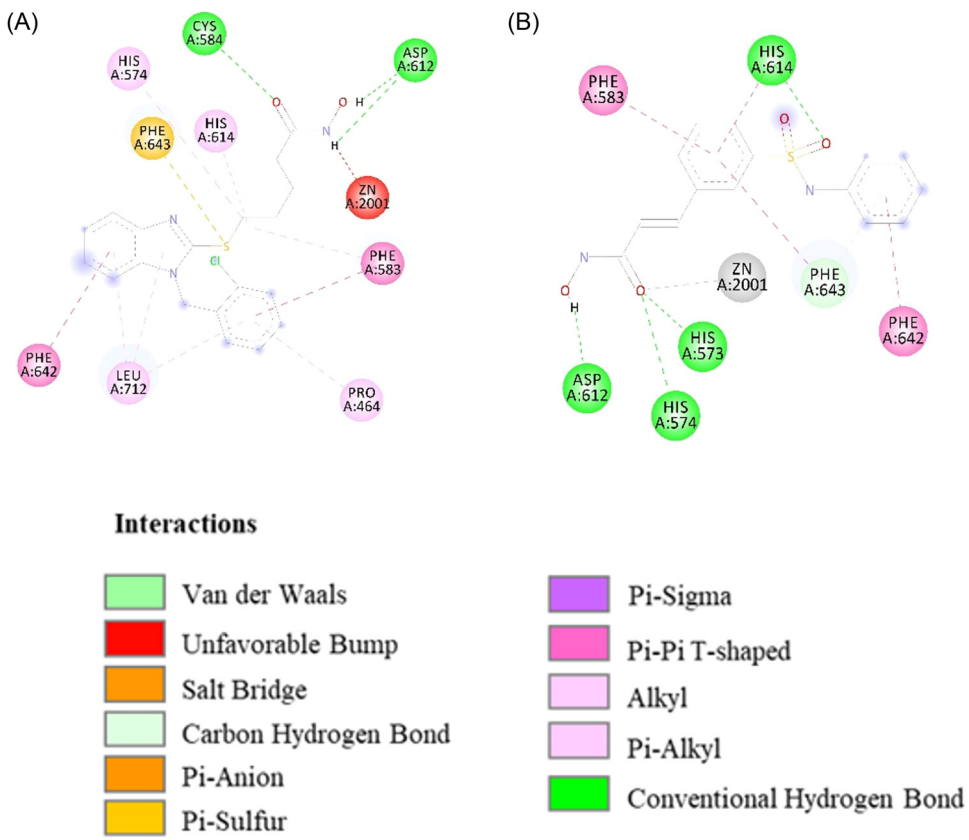

Fig. 5 Docking conformation of compound **7** and belinostat with HDACs enzyme. (A) Docking pose of compound **7** with HDAC6; (B) docking pose of belinostat with HDAC6.

compound 7 had the highest binding affinity toward HDAC6 among the investigated HDAC enzymes (−8.46 kcal mol^{-1}), which was higher than that of the reference ligand (belinostat). Docking pose analysis further revealed the H-bond interactions with the key residues Cys584 and Asp612 in the binding region of HDAC6. Thus, compound 7 could serve as a promising candidate to selectively inhibit HDAC6 enzyme activity.

Data availability

All the data used to support the finding of this study are included within the article. All other data are available from the corresponding author upon request.

Author contributions

Hong Phuong Nguyen, Su-Geun Yang and Bui Thi Buu Hue conceived the idea and designed the works. Bui Thi Buu Hue, Le Trong Hieu, Hong Vinh Quang, Nguyen Phu Quy, and Quang De Tran performed chemical synthesis, purification, and structure identification. Dang Minh Quan, Cuong Quoc Nguyen and Quang De Tran performed molecular docking studies. Hong Phuong Nguyen, Tran Phuong Hoa, Hosun Jung, and Su-Geun Yang performed, analyzed and supervised biological assays. Hong Phuong Nguyen, Bui Thi Buu Hue, Dang Minh Quan, Su-Geun Yang wrote, prepared, and edited the original draft. All authors have approved the final version of the manuscript.

Conflicts of interest

No potential conflict of interest was reported by the authors.

Acknowledgements

This work was supported by the Ministry of Education and Training of Vietnam under grant number B2020-TCT-12. This work was also supported by the Basic Science Research Program and the Brain Pool program of the National Research Foundation (NRF) funded by the Korean government (MOE and MSIT) (2018R1A6A1A03025523 and RS-2023-00208587) and the Young Medical-Scientist Research Grant Program funded by Daewoong Foundation (DFY2203P).

References

1 M. A. Dawson and T. Kouzarides, Cancer epigenetics: from mechanism to therapy, *Cell*, 2012, **150**(1), 12–27.
2 M. Mottamal, S. Zheng, T. L. Huang and G. Wang, Histone deacetylase inhibitors in clinical studies as templates for new anticancer agents, *Molecules*, 2015, **20**(3), 3898–3941.
3 (*a*) K. Kashyap and R. Kakkar, Exploring structural requirements of isoform selective histone deacetylase inhibitors: a comparative in silico study, *J. Biomol. Struct. Dyn.*, 2021, **39**(2), 502–517; (*b*) Y. Zhang and W. Xu, Isoform-selective histone deacetylase inhibitors: the trend and promise of disease treatment, *Epigenomics*, 2015, **7**(1), 5–7.
4 E. Pontiki and D. Hadjipavlou-Litina, Histone deacetylase inhibitors (HDACIs). Structure–activity relationships: history and new QSAR perspectives, *Med. Res. Rev.*, 2012, **32**(1), 1–165.
5 (*a*) J. M. Wagner, B. Hackanson, M. Lubbert and M. Jung, Histone deacetylase (HDAC) inhibitors in recent clinical trials for cancer therapy, *Clin. Epigenet.*, 2010, **1**(3–4), 117–136; (*b*) J. Vansteenkiste, E. Van Cutsem, H. Dumez, C. Chen, J. L. Ricker, S. S. Randolph and P. Schoffski, Early phase II trial of oral vorinostat in relapsed or refractory breast, colorectal, or non-small cell lung cancer, *Invest. New Drugs*, 2008, **26**(5), 483–488; (*c*) P. Richardson, C. Mitsiades, K. Colson, E. Reilly, L. McBride, J. Chiao, L. Sun, J. Ricker, S. Rizvi, C. Oerth, B. Atkins, I. Fearen, K. Anderson and D. Siegel, Phase I trial of oral vorinostat (suberoylanilide hydroxamic acid, SAHA) in patients with advanced multiple myeloma, *Leuk. Lymphoma*, 2008, **49**(3), 502–507; (*d*) M. Crump, B. Coiffier, E. D. Jacobsen, L. Sun, J. L. Ricker, H. Xie, S. R. Frankel, S. S. Randolph and B. D. Cheson, Phase II trial of oral vorinostat (suberoylanilide hydroxamic acid) in relapsed diffuse large-B-cell lymphoma, *Ann. Oncol.*, 2008, **19**(5), 964–969; (*e*) M. Duvic, R. Talpur, X. Ni, C. Zhang, P. Hazarika, C. Kelly, J. H. Chiao, J. F. Reilly, J. L. Ricker, V. M. Richon and S. R. Frankel, Phase 2 trial of oral vorinostat (suberoylanilide hydroxamic acid, SAHA) for refractory cutaneous T-cell lymphoma (CTCL), *Blood*, 2007, **109**(1), 31–39; (*f*) F. Thaler and C. Mercurio, Towards selective inhibition of histone deacetylase isoforms: what has been achieved, where we are and what will be next, *ChemMedChem*, 2014, **9**(3), 523–526.
6 Z. Yang, T. Wang, F. Wang, T. Niu, Z. Liu, X. Chen, C. Long, M. Tang, D. Cao, X. Wang, W. Xiang, Y. Yi, L. Ma, J. You and L. Chen, Discovery of Selective Histone Deacetylase 6 Inhibitors Using the Quinazoline as the Cap for the Treatment of Cancer, *J. Med. Chem.*, 2016, **59**(4), 1455–1470.
7 (*a*) M. Haberland, R. L. Montgomery and E. N. Olson, The many roles of histone deacetylases in development and physiology: implications for disease and therapy, *Nat. Rev. Genet.*, 2009, **10**(1), 32–42; (*b*) O. Witt, H. E. Deubzer, T. Milde and I. Oehme, HDAC family: What are the cancer relevant targets?, *Cancer Lett.*, 2009, **277**(1), 8–21.
8 J. E. Bradner, N. West, M. L. Grachan, E. F. Greenberg, S. J. Haggarty, T. Warnow and R. Mazitschek, Chemical phylogenetics of histone deacetylases, *Nat. Chem. Biol.*, 2010, **6**(3), 238–243.
9 (*a*) V. D. Kekatpure, A. J. Dannenberg and K. Subbaramaiah, HDAC6 modulates Hsp90 chaperone activity and regulates activation of aryl hydrocarbon receptor signaling, *J. Biol. Chem.*, 2009, **284**(12), 7436–7445; (*b*) C. Hubbert, A. Guardiola, R. Shao, Y. Kawaguchi, A. Ito, A. Nixon, M. Yoshida, X. F. Wang and T. P. Yao, HDAC6 is a microtubule-associated deacetylase, *Nature*, 2002, **417**(6887), 455–458; (*c*) J. Schemies, W. Sippl and M. Jung, Histone deacetylase inhibitors that target tubulin, *Cancer Lett.*, 2009, **280**(2), 222–232.
10 N. Govindarajan, P. Rao, S. Burkhardt, F. Sananbenesi, O. M. Schluter, F. Bradke, J. Lu and A. Fischer, Reducing

HDAC6 ameliorates cognitive deficits in a mouse model for Alzheimer's disease, *EMBO Mol. Med.*, 2013, **5**(1), 52–63.

11 (*a*) C. Seidel, M. Schnekenburger, M. Dicato and M. Diederich, Histone deacetylase 6 in health and disease, *Epigenomics*, 2015, **7**(1), 103–118; (*b*) J. H. Kalin and J. A. Bergman, Development and therapeutic implications of selective histone deacetylase 6 inhibitors, *J. Med. Chem.*, 2013, **56**(16), 6297–6313.

12 (*a*) X. Lin, W. Chen, Z. Qiu, L. Guo, W. Zhu, W. Li, Z. Wang, W. Zhang, Z. Zhang, Y. Rong, M. Zhang, L. Yu, S. Zhong, R. Zhao, X. Wu, J. C. Wong and G. Tang, Design and synthesis of orally bioavailable aminopyrrolidinone histone deacetylase 6 inhibitors, *J. Med. Chem.*, 2015, **58**(6), 2809–2820; (*b*) C. L. Hamblett, J. L. Methot, D. M. Mampreian, D. L. Sloman, M. G. Stanton, A. M. Kral, J. C. Fleming, J. C. Cruz, M. Chenard, N. Ozerova, A. M. Hitz, H. Wang, S. V. Deshmukh, N. Nazef, A. Harsch, B. Hughes, W. K. Dahlberg, A. A. Szewczak, R. E. Middleton, R. T. Mosley, J. P. Secrist and T. A. Miller, The discovery of 6-amino nicotinamides as potent and selective histone deacetylase inhibitors, *Bioorg. Med. Chem. Lett.*, 2007, **17**(19), 5300–5309.

13 (*a*) D. Diedrich, A. Hamacher, C. G. Gertzen, L. A. Alves Avelar, G. J. Reiss, T. Kurz, H. Gohlke, M. U. Kassack and F. K. Hansen, Rational design and diversity-oriented synthesis of peptoid-based selective HDAC6 inhibitors, *Chem. Commun.*, 2016, **52**(15), 3219–3222; (*b*) S. Shen, V. Benoy, J. A. Bergman, J. H. Kalin, M. Frojuello, G. Vistoli, W. Haeck, L. Van Den Bosch and A. P. Kozikowski, Bicyclic-Capped Histone Deacetylase 6 Inhibitors with Improved Activity in a Model of Axonal Charcot-Marie-Tooth Disease, *ACS Chem. Neurosci.*, 2016, **7**(2), 240–258; (*c*) C. A. Simoes-Pires, P. Bertrand and M. Cuendet, Novel histone deacetylase 6 (HDAC6) selective inhibitors: a patent evaluation (WO2014181137), *Expert Opin. Ther. Pat.*, 2017, **27**(3), 229–236; (*d*) Y. Hai and D. W. Christianson, Histone deacetylase 6 structure and molecular basis of catalysis and inhibition, *Nat. Chem. Biol.*, 2016, **12**(9), 741–747; (*e*) Y. Miyake, J. J. Keusch, L. Wang, M. Saito, D. Hess, X. Wang, B. J. Melancon, P. Helquist, H. Gut and P. Matthias, Structural insights into HDAC6 tubulin deacetylation and its selective inhibition, *Nat. Chem. Biol.*, 2016, **12**(9), 748–754; (*f*) N. J. Porter, A. Mahendran, R. Breslow and D. W. Christianson, Unusual zinc-binding mode of HDAC6-selective hydroxamate inhibitors, *Proc. Natl. Acad. Sci. U. S. A.*, 2017, **114**(51), 13459–13464.

14 T. Wang, M. Sepulveda, P. Gonzales and S. Gately, Identification of novel HDAC inhibitors through cell based screening and their evaluation as potential anticancer agents, *Bioorg. Med. Chem. Lett.*, 2013, **23**(17), 4790–4793.

15 C. Mantzourani, D. Gkikas, A. Kokotos, P. Nummela, M. A. Theodoropoulou, K. C. Wu, D. P. Fairlie, P. K. Politis, A. Ristimaki and G. Kokotos, Synthesis of benzoxazole-based vorinostat analogs and their antiproliferative activity, *Bioorg. Chem.*, 2021, **114**, 105132.

16 S. E. Kassab, S. Mowafy, A. M. Alserw, J. A. Seliem, S. M. El-Naggar, N. N. Omar and M. M. Awad, Structure-based design generated novel hydroxamic acid based preferential HDAC6 lead inhibitor with on-target cytotoxic activity against primary choroid plexus carcinoma, *J. Enzyme Inhib. Med. Chem.*, 2019, **34**(1), 1062–1077.

17 (*a*) Y. Bansal and O. Silakari, The therapeutic journey of benzimidazoles: a review, *Bioorg. Med. Chem.*, 2012, **20**(21), 6208–6236; (*b*) T. B. H. Bui, H. M. Nguyen, V. H. Mai, L. D. T. Danh, H. S. Nguyen, Q. D. Tran and H. Morita, Facile Sodium Metabisulfite Mediated Synthesis of 1,2-Disubstituted Benzimidazoles and Cytotoxicity Evaluation, *Heterocycles*, 2019, **98**(5), 650–665.

18 L. L. C. Schrodinger, *The PyMOL Molecular Graphics System, Version 1.3r1*, 2010.

19 M. J. Frisch, G. W. Trucks, H. B. Schlegel, G. E. Scuseria, M. A. Robb, J. R. Cheeseman, G. Scalmani, V. Barone, G. A. Petersson, H. Nakatsuji, X. Li, M. Caricato, A. V. Marenich, J. Bloino, B. G. Janesko, R. Gomperts, B. Mennucci, H. P. Hratchian, J. V. Ortiz, A. F. Izmaylov, J. L. Sonnenberg, Williams, F. Ding, F. Lipparini, F. Egidi, J. Goings, B. Peng, A. Petrone, T. Henderson, D. Ranasinghe, V. G. Zakrzewski, J. Gao, N. Rega, G. Zheng, W. Liang, M. Hada, M. Ehara, K. Toyota, R. Fukuda, J. Hasegawa, M. Ishida, T. Nakajima, Y. Honda, O. Kitao, H. Nakai, T. Vreven, K. Throssell, J. A. Montgomery Jr., J. E. Peralta, F. Ogliaro, M. J. Bearpark, J. J. Heyd, E. N. Brothers, K. N. Kudin, V. N. Staroverov, T. A. Keith, R. Kobayashi, J. Normand, K. Raghavachari, A. P. Rendell, J. C. Burant, S. S. Iyengar, J. Tomasi, M. Cossi, J. M. Millam, M. Klene, C. Adamo, R. Cammi, J. W. Ochterski, R. L. Martin, K. Morokuma, O. Farkas, J. B. Foresman and D. J. Fox, *Gaussian 09 Rev. d.01*, Wallingford, CT, 2009.

20 M. T. Buckley, J. Yoon, H. Yee, L. Chiriboga, L. Liebes, G. Ara, X. Qian, D. F. Bajorin, T.-T. Sun, X.-R. Wu and I. Osman, The histone deacetylase inhibitor belinostat (PXD101) suppresses bladder cancer cell growth *in vitro* and *in vivo*, *J. Transl. Med.*, 2007, **5**(1), 49–60.

21 P. J. Watson, L. Fairall, G. M. Santos and J. W. R. Schwabe, Structure of HDAC3 bound to co-repressor and inositol tetraphosphate, *Nature*, 2012, **481**(7381), 335–340.

22 R. W. Bürli, C. A. Luckhurst, O. Aziz, K. L. Matthews, D. Yates, K. A. Lyons, M. Beconi, G. McAllister, P. Breccia, A. J. Stott, S. D. Penrose, M. Wall, M. Lamers, P. Leonard, I. Müller, C. M. Richardson, R. Jarvis, L. Stones, S. Hughes, G. Wishart, A. F. Haughan, C. O'Connell, T. Mead, H. McNeil, J. Vann, J. Mangette, M. Maillard, V. Beaumont, I. Munoz-Sanjuan and C. Dominguez, Design, Synthesis, and Biological Evaluation of Potent and Selective Class IIa Histone Deacetylase (HDAC) Inhibitors as a Potential Therapy for Huntington's Disease, *J. Med. Chem.*, 2013, **56**(24), 9934–9954.

23 Y. Hai and D. W. Christianson, Histone deacetylase 6 structure and molecular basis of catalysis and inhibition, *Nat. Chem. Biol.*, 2016, **12**(9), 741–747.

24 J. R. Somoza, R. J. Skene, B. A. Katz, C. Mol, J. D. Ho, A. J. Jennings, C. Luong, A. Arvai, J. J. Buggy, E. Chi, J. Tang, B. C. Sang, E. Verner, R. Wynands, E. M. Leahy,

D. R. Dougan, G. Snell, M. Navre, M. W. Knuth, R. V. Swanson, D. E. McRee and L. W. Tari, Structural snapshots of human HDAC8 provide insights into the class I histone deacetylases, *Structure*, 2004, **12**(7), 1325–1334.

25 D. Santos-Martins, S. Forli, M. J. Ramos and A. J. Olson, AutoDock4Zn: An Improved AutoDock Force Field for Small-Molecule Docking to Zinc Metalloproteins, *J. Chem. Inf. Model.*, 2014, **54**(8), 2371–2379.

26 B. T. B. Hue, P. H. Nguyen, T. Q. De, M. Van Hieu, E. Jo, N. Van Tuan, T. T. Thoa, L. D. Anh, N. H. Son, D. La Duc Thanh, M. Dupont-Rouzeyrol, R. Grailhe and M. P. Windisch, Benzimidazole Derivatives as Novel Zika Virus Inhibitors, *ChemMedChem*, 2020, **15**(15), 1453–1463.

27 L. Yang, X. Xue and Y. Zhang, Simple and Efficient Synthesis of Belinostat, *Synth. Commun.*, 2010, **40**, 2520–2524.

28 (*a*) N. T. Dan, H. D. Quang, V. Van Truong, D. Huu Nghi, N. M. Cuong, T. D. Cuong, T. Q. Toan, L. G. Bach, N. H. T. Anh, N. T. Mai, N. T. Lan, L. Van Chinh and P. M. Quan, Design, synthesis, structure, in vitro cytotoxic activity evaluation and docking studies on target enzyme GSK-3beta of new indirubin-3′-oxime derivatives, *Sci. Rep.*, 2020, **10**(1), 11429–11441; (*b*) S. T. Ngo, N. M. Tam, M. Q. Pham and T. H. Nguyen, Benchmark of Popular Free Energy Approaches Revealing the Inhibitors Binding to SARS-CoV-2 Mpro, *J. Chem. Inf. Model.*, 2021, **61**(5), 2302–2312; (*c*) N. T. Nguyen, T. H. Nguyen, T. N. H. Pham, N. T. Huy, M. V. Bay, M. Q. Pham, P. C. Nam, V. V. Vu and S. T. Ngo, Autodock Vina Adopts More Accurate Binding Poses but Autodock4 Forms Better Binding Affinity, *J. Chem. Inf. Model.*, 2020, **60**(1), 204–211.

29 Q. A. Ngo, T. H. N. Thi, M. Q. Pham, D. Delfino and T. T. Do, Antiproliferative and antiinflammatory coxib-combretastatin hybrids suppress cell cycle progression and induce apoptosis of MCF7 breast cancer cells, *Mol. Diversity*, 2021, **25**(4), 2307–2319.

30 G. Ortore, F. D. Colo and A. Martinelli, Docking of Hydroxamic Acids into HDAC1 and HDAC8: A Rationalization of Activity Trends and Selectivities, *J. Chem. Inf. Model.*, 2009, **49**(12), 2774–2785.

31 R. Laskowski, J. A. C. Rullmann, M. W. MacArthur, R. Kaptein and J. M. Thornton, AQUA and PROCHECK-NMR: Programs for checking the quality of protein structures solved by NMR, *J. Biomol. NMR*, 1996, **8**, 477–486.